HETEROCYCLES, Vol. 87, No. 2, 2013, pp. 319 - 328. © 2013 The Japan Institute of Heterocyclic Chemistry
Received, 9th November, 2012, Accepted, 13th December, 2012, Published online, 21st December, 2012
DOI: 10.3987/COM-12-12623

ROLE OF CH/O AND CH/π INTERACTIONS IN STRUCTURAL STABILITY. EFFECT ON *ENDO* SELECTIVITY IN 1,3-DIPOLAR REACTION OF ELECTRON-DEFICIENT 4-OXO-4*H*-PYRAZOLE 1,2-DIOXIDES WITH *N*-SUBSTITUTED MALEIMIDES

Koki Yamaguchi, Kazunobu Harano, and Masashi Eto*

Faculty of Pharmaceutical Sciences, Sojo University, 4-22-1 Ikeda, Kumamoto 860-0082, Japan (meto@ph.sojo-u.ac.jp)

Abstract – The molecular structure of the 1:2 cycloadduct derived from 1,3-dipolar reaction of 3,5-bis(methoxycarbonyl)-4-oxo-4*H*-pyrazole 1,2-dioxide (**1a**) with *N*-phenyl maleimide (**2a**) was established to be an *anti-endo-endo* form by the single crystal X-ray analysis. The weak attractive CH/O interaction between **1a** and **2a** is conjectured to play an important role in the preferential formation of the *endo* transition-state. The formation mechanism of the adduct is discussed on the basis of transition-state structures optimized at the B3LYP/6-31G(d) level of theory.

INTRODUCTION

3,5-Disubstituted 4-oxo-4*H*-pyrazole 1,2-dioxide (**1**), which contains two nitrone moieties, undergoes 1,3-dipolar cycloaddition with various unsaturated compounds to give 1:1 cycloadducts.[1,2] Usually, the remaining nitrone moiety is unreactive towards cycloaddition with excess dienophiles.[1b] In spite of the existence of an additional nitrone moiety in **1**, formation of the 1:2 cycloadducts is yet to be reported. However, preliminary density functional theory (DFT) calculations for the model reaction of **1** with ethylene estimate that the reaction barrier in the secondary reaction is marginally higher than that of the primary reaction.[1g] This suggests that the possibility of cycloaddition between the remaining 1,3-dipole and ethylene moiety exists.

During the study of the reaction behaviour of **1**, we isolated unexpectedly the heterocage compound produced by the sequential 1,3-dipolar reactions (involving an initial intermolecular cycloaddition and the subsequently successive intramolecular cycloaddition) of 3,5-bis(methoxycarbonyl)-4-oxo-4*H*-pyrazole 1,2-dioxide (**1a**) containing electron-deficient substituents with 1,3,5-cycloheptatriene (Scheme 1).[1g] This

result prompted us to reinvestigate the reaction behaviour of **1** towards planar cyclic olefins to obtain a corresponding 1:2 cycloadduct. In this paper, we report the reaction behaviour of **1** towards *N*-substituted maleimides (**2**) and furnish the first example of the formation of the 1:2 cycloadduct.

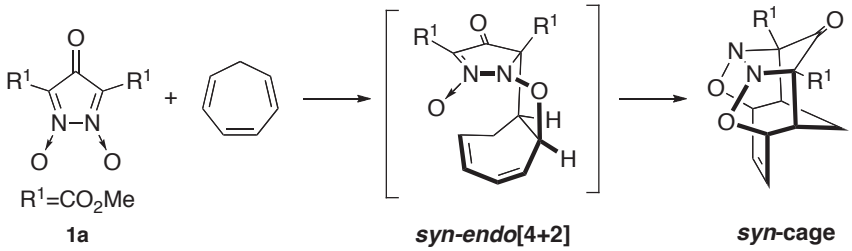

Scheme 1

RESULTS AND DISCUSSION

A mixture of **1a** and *N*-phenylmaleimide (**2a**) in benzene was refluxed for 23 h to give a mixture of 1:1 cycloadducts (*endo*-**3aa**, 17% and *exo*-**3aa**, 10%), 1:2 cycloadduct (**4aa**, 22%), and isoxazole derivative (**5aa**, 1%) as shown in Scheme 2 and Table 1. The MS, ^{1}H-NMR and ^{13}C-NMR spectra of **3aa** and **4aa** were consistent with the 1:1 and 1:2 1,3-dipolar cycloaddition products, respectively. The *endo*/*exo* structures of **3aa** were determined by comparing the NMR spectra. In *exo*-**3aa**, two methine protons (δ4.44 and 5.49) resonate at high-field regions when compared to those of the *endo* isomer (δ4.79 and 5.90), owing to the ring current effect of the R–C=N→O moiety.[1b]

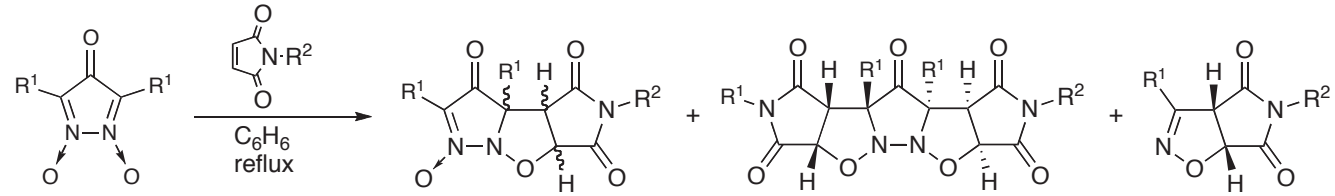

Scheme 2

Table 1. Reaction conditions and products for the reaction of dioxides (**1**) with *N*-substituted maleimides (**2**).

Exp. No.	dioxides	maleimides	time (h)	product yield (%)			
				1:1 adducts		1:2 adduct	isoxazole
1	**1a**	**2a**	23	17 (*endo*-**3aa**)	10 (*exo*-**3aa**)	22 (**4aa**)	1 (**5aa**)
2[a)]		**2b**	24	32 (*endo*-**3ab**)		20 (**4ab**)	7 (**5ab**)
3[b)]	**1b**	**2a**	23	36 (*endo*-**3ba**)	23 (*exo*-**3ba**)		
4[c)]		**2b**	20	36 (*endo*-**3bb**)	23 (*exo*-**3bb**)		

a) recovery of **1a**, 16%; b) recovery of **1b**, 17%; c) recovery of **1b**, 4%

Immediately after separation of **3aa** by silica gel column chromatography, the *endo*/*exo* ratio was approximately 3:2. However, the amount of *endo*-form increased with time, suggesting that the isomerization from the *exo*-form to the *endo*-form gradually occurred in the solution (DMSO, acetone, or $CHCl_3$). Interestingly, the colouration of the solution was observed during the course of the reaction. The spectra showed a maximum absorption in the vicinity of 600 nm. The visible absorption spectrum of the reaction mixture was not merely a cumulative result obtained by the addition of the spectra of the pure samples of the **1a** and **2a**, indicating the presence of a charge-transfer (CT) complex between **1a** and **2a** (Figure 1).

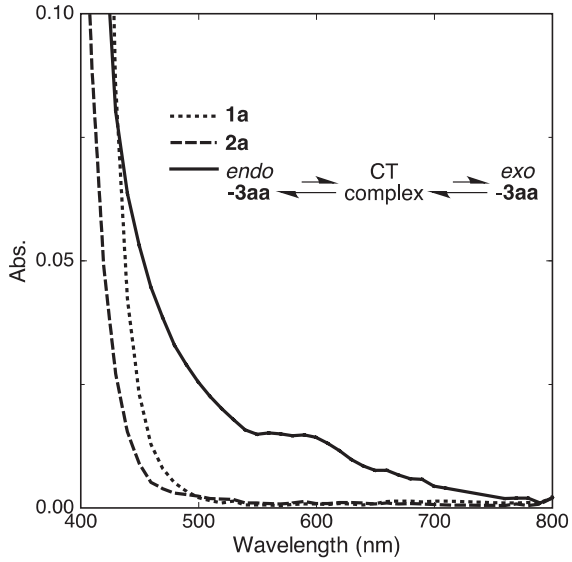

Figure 1. Visible absorption spectrum of equilibrium reaction between *endo*-**3aa** and *exo*-**3aa** (in $CHCl_3$)

The ^{1}H-NMR and ^{13}C-NMR spectra of the 1:2 cycloadduct (**4aa**) indicated a highly symmetrical structure. Six stereoisomers of **4aa** are possible with respect to the combination of *endo*/*exo* selectivity and *syn*/*anti* approach to the 1:1 cycloadduct (Figure 2). In the ^{1}H-NMR spectrum of **4aa**, a high-field shifted methyl signal of the methoxycarbonyl group was observed at δ3.14 due to the anisotropy of the *N*-phenyl group, in comparison with that of the 1:1 cycloadduct of **1a** and **2a** (δ3.78). This observation suggests that the orientation of the cycloaddition was the *anti-endo-endo* form. As shown in Figure 3, the structure of **4aa** was established to be an *anti-endo-endo* 1:2 cycloadduct by the single crystal X-ray analysis, in which the N–N bond length and O–N–N–O dihedral angle were found to be 1.502(3) Å and 86.4(1)°, respectively. The S-shaped structure indicates that the cycloadditions at both stages proceeded through *endo* transition states. The analysis also suggests the presence of the CH/π interaction[3] between the methyl hydrogen of the ester group and the phenyl ring, in which the nearest H_3C•••C distance was 3.453(5) Å. A similar close contact was found between another ester group and the phenyl ring of the adjacent molecule [with H_3C•••C distance of 3.506(4) Å]. To the

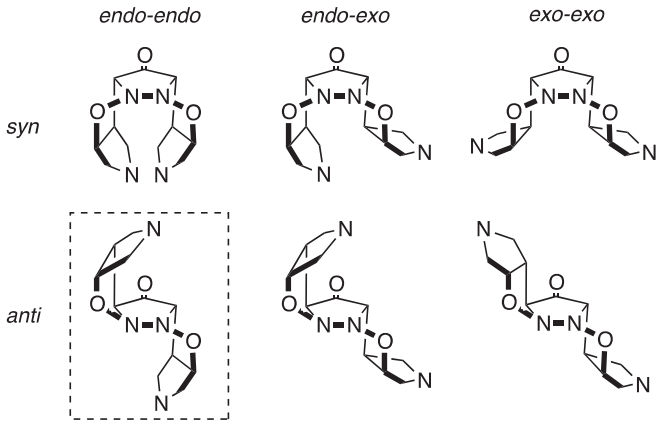

Figure 2. Possible six stereoisomers of 1:2 cycloadduct of **4aa** (substituents are omitted)

best of our knowledge, this is the first demonstration of isolation of a 1:2 cycloadduct in the 1,3-dipolar cycloaddition of **1** with dipolarophiles.

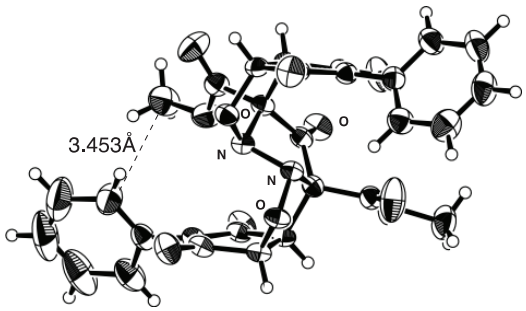

Figure 3. ORTEP drawing of *anti-endo-endo*-**4aa**

The formation of the 1:2 cycloadduct (**4aa**) is attributed to the effective contribution of the neutral-type FMO interaction according to Sustmann's classification[4] of cycloadditions. The first step of the cycloaddition is controlled by the inverse-type interaction[1b] (i.e., by the combination of LUMO of **1a** and HOMO of **2a**). However, the second step is a neutral-type reaction, wherein both the HOMO/LUMO and LUMO/HOMO interactions are operative.

Similarly, **1a** reacted with *N*-methyl maleimide (**2b**) to produce a 1:1 cycloadduct (*endo*-**3ab**, 32%) and a 1:2 cycloadduct (**4ab**, 20%) with the remnant reactant recovered. The stereochemistry of **4ab** was confirmed and the product exhibited an *anti-endo-endo* form, which was inferred based on the similarity of the methine proton signals of **4aa**.

In the reactions of **1a** with **2**, minor products (**5aa** or **5ab**) were also obtained. The structure of **5aa** was determined to be a dihydroisoxazole derivative based on the X-ray structure of **5ab**. The derivative is probably produced from the extrusion of the carbonyl group of a 1:2 cycloadduct assisted by the weakened N–N and (O=)C–C(CO_2Me) bonds.

In contrast to the reaction behaviour of **1a** containing electron-deficient substituents, the reactions of the diphenyl derivative (**1b**) with **2** produced an *endo*/*exo* mixture of exclusively the 1:1 cycloadduct (*endo*-**3ba**, 36% and *exo*-**3ba**, 23%).[5]

In order to evaluate the differences between the reaction behaviours of **1a** and **1b** toward **2**, DFT[6] calculations at the B3LYP/6-31G(d) level were performed on the possible reaction pathways of **1** with **2b** (Figure 4). For the primary step of the reaction between **1a** and **2b**, the GS energy of *endo*-**3ab** is found to be much smaller than that of *exo*-**3ab**, indicating the lower thermodynamic stability of the *exo* cycloadduct. In contrast to **1a**, the ground-state (GS) energy of the *exo* adduct derived from the model reaction of the unsubstituted 4-oxo-4*H*-pyrazole 1,2-dioxide (**1c**) with **2a** is 3.2 kcal/mol more stable than that of the *endo* product.[7] The stability of *endo*-**3ab** could be attributed to the C–H/O=C< type interaction[8] between the C3b-methine proton and the oxygen atom of the ester group (with the CH•••O distance of 2.304 Å). The transition-state (TS) calculation also suggested the contribution of intermolecular CH/O interaction (with the CH•••O distance of 2.504 Å) to the stabilization of the *endo*-TS, which is more stable than the *exo*-TS.[9] The energy difference between two TS is 0.8 kcal/mol, which supports the observed *endo*/*exo* selectivity. Changing the substituent on nitrogen of maleimide from methyl to phenyl

group may increase the steric congestion between the *N*-substituent and the ester group of **1a** in the transition structure, resulting in a decrease in the preferential formation of the *endo*-TS in the primary reaction step between **1a** and **2a**.[10]

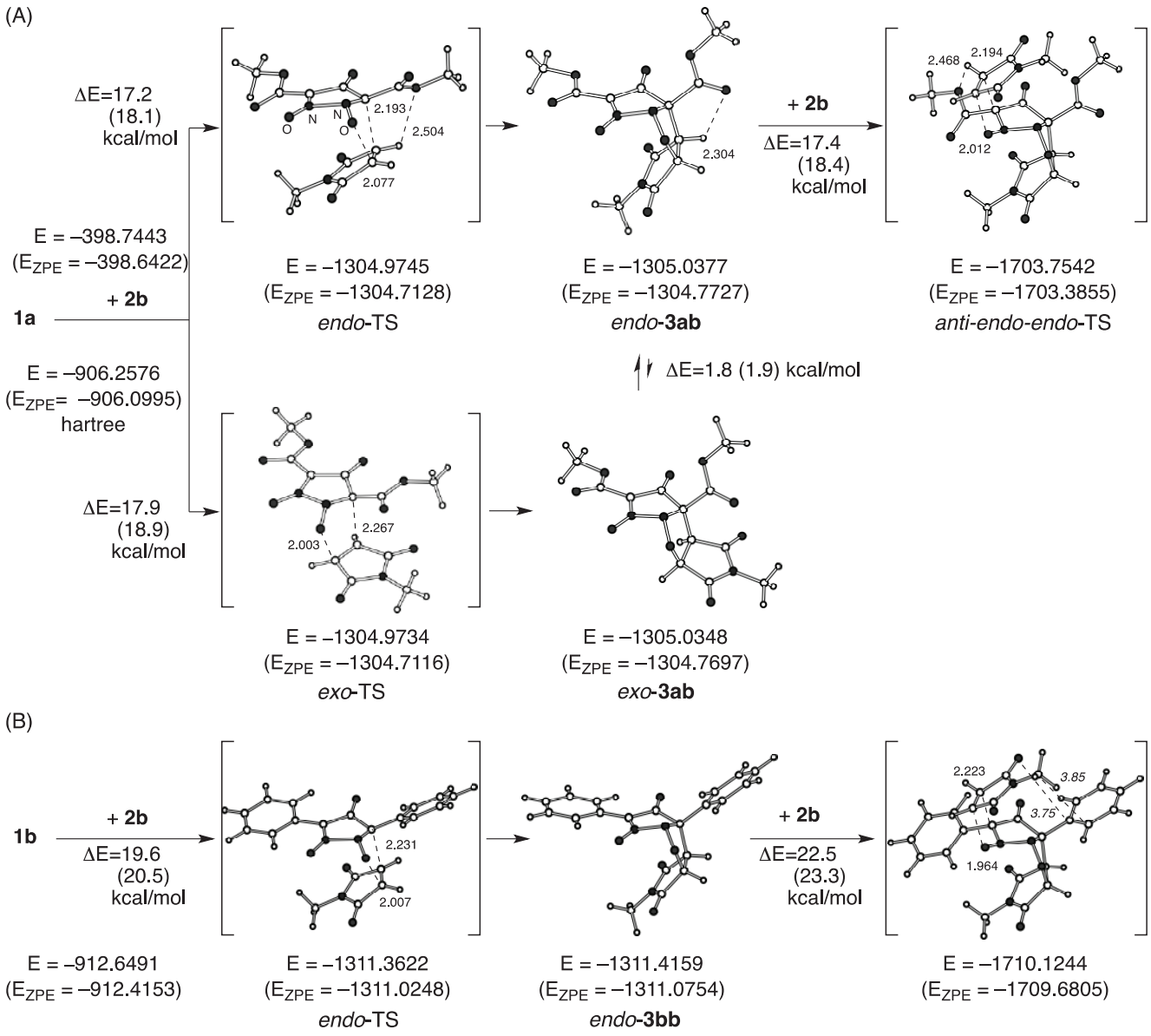

Figure 4. B3LYP/6-31G(d)-calculated reaction barriers for the formation reaction of the 1:1 and 1:2 cycloadducts: (A) reaction of **1a** and **2b** (B) reaction of **1b** and **2b** (zero point energy corrected values are shown in parentheses)

The secondary TS energy of the cycloaddition of **1b** toward **2b** is 23.3 kcal/mol, which is ca. 3 kcal/mol higher than that of the primary reaction step, as shown in Figure 4. For the reaction of **1a** with **2b,** the reaction barrier of the secondary step seems almost identical to that of the initial step. These calculations strongly suggest that the successive cycloaddition between the remaining 1,3-dipole of **3ab** and **2b** is possible. The difference in the secondary reaction barriers of *endo*-**3ab** and *endo*-**3bb** can be accounted

on the basis of steric interferences and an attractive CH/O interaction between the substituents of the addends in the TS structures. The distance between the methine hydrogen adjacent to the carbonyl group and the ester oxygen atom on the ester group in the secondary TS structure of **3ab** is 2.468Å, which seems to contribute the stabilization of the *anti-endo-endo*-TS (Figure 4). The TS energy is ca. 1.6 kcal/mol lower than that of the model rotated around the C–CO_2Me bond without CH/O interaction.[11] These calculations indicate that the CH/O interaction between **1a** and **2** could play an important role in the preferential formation of the *endo*-TS.[12]

On the other hands, considering that the formation of the *exo*-**3ab** adduct, the formation of *anti-endo-exo*-**3ab** may be expected. However, the *endo* approach of **2b** against *exo*-**3ab** might be unfavourable even if the contribution of the CH/O interaction exists. This is due to the steric interference between *N*-Me and the flexibility restricted C3a-CO_2Me group by the *exo*-protruded maleimide ring.

In summary, the *anti-endo-endo*-1:2 cycloadduct was formed by the sequential 1,3-dipolar reactions of **1a** containing electron-withdrawing substituents with maleimides (**2**). In these reactions, the weak attractive CH/O interaction in the TS affected the stereoselectivity of the 1,3-dipolar cycloadditon.

EXPERIMENTAL

Melting points were uncorrected. The IR spectra were taken with a Hitachi 270-30 spectrophotometer. ^{1}H-NMR and ^{13}C-NMR spectra were taken with JEOL JNM-EX 270 (270 MHz) and JNM-A 500 (500 MHz) spectrometers for ca.10% solution with TMS as an internal standard; chemical shifts are expressed as δ values and the coupling constants (*J*) are expressed in Hz. Mass spectra were obtained using a JEOL JMS-T100LC Accu TOF instrument.

Reaction of 1 with 2 (general procedure) – A solution of 0.6 g (2.5 mmol) of **la** in 10 mL of benzene and 0.87 g of **2a** was heated under reflux for 23 h. The mixture was cooled and the solvent was removed under vacuum. The residue was chromatographed on silica gel. The products separated were crystallized from appropriate solvents.

endo-**3aa**: colorless prisms; mp 175–180 °C (from acetone); IR (KBr) 1773, 1728 cm^{-1}; ^{1}H-NMR (500 MHz, DMSO-d_6) δ: 3.78 (s, CO_2CH_3, 3H), 3.91 (s, CO_2CH_3, 3H), 4.79 (d, *J* = 8.0, 1H, C3b-H), 5.90 (d, *J* = 8.0, 1H, C6a-H), 6.97 (d, *J* = 7.5, 1H, Ar-H), 7.27 (d, *J* = 6.9, 1H, Ar-H), 7.47–7.56 (m, 3H, Ar-H); ^{13}C-NMR (125 MHz, DMSO-d_6) δ: 53.1 (C3b), 53.9 (CO_2CH_3), 54.8 (CO_2CH_3), 85.8 (C6a), 83.3 (*C*-COO), 114.6 (C2), 155.0 (*C*OO), 162.7 (*C*OO), 169.6 (NC=O), 169.9 (NC=O), 177.9 (C=O); HRMS (ESI) Calcd. for $C_{18}H_{17}N_3O_{10}Na$ (M^++CH_3OH+Na): 458.08116. Found: 458.08268.

exo-**3aa**: obtained as an *endo*/*exo* mixture; ^{1}H-NMR (500 MHz, DMSO-d_6) δ: 3.75 (s, 3H, CO_2CH_3), 3.84 (s, 3H, CO_2CH_3), 4.44 (d, *J* = 7.5, 1H, C3b-H), 5.49 (d, *J* = 7.5, 1H, C6a-H), 6.97 (d, *J* = 7.5, 1H, Ar-H), 7.47–7.56 (m, 4H, Ar-H); ^{13}C-NMR (125 MHz, DMSO-d_6) δ: 52.5 (CO_2CH_3), 52.6 (CO_2CH_3),

54.4 (C3b), 79.1 (*C*-COO), 83.4 (C6a), 117.1 (C2), 156.0 (*C*OO), 162.2 (*C*OO), 168.1 (NC=O), 170.3 (NC=O), 180.7 (C=O).

anti-endo-endo-**4aa**: colorless prisms; mp 229–230 °C (from acetone-$CHCl_3$); IR (KBr) 1724 cm^{-1}; ^{1}H-NMR (500 MHz, DMSO-d_6) δ: 3.14 (s, 3H, CO_2CH_3), 4.59 (d, *J* = 8.0, 1H, >CH-C(=O)), 5.56 (d, *J* = 8.0, 1H, -OCH-C(=O)), 7.29 (d, *J* = 7.5, 2H, ArH), 7.45 (dd, *J* = 7.5, 7.5, 1H, ArH), 7.56 (dd, *J* = 7.5, 7.5, 2H, ArH); ^{13}C-NMR (125 MHz, DMSO-d_6) δ 53.7 (>*C*H-C(=O)), 54.0 (COO*C*H_3), 81.0 (-O*C*H-C(=O)), 84.0 (*C*-COO), 162.2 (COO), 170.4 (NC=O), 172.1 (NC=O), 183.0 (C=O); *m/z* (FAB): 577 (M^++1). Anal. Calcd for $C_{27}H_{20}N_4O_{11}$ + C_3H_6O (Acetone): C, 56.78; H, 4.13; N, 8.83. Found: C, 56.69; H, 3.89; N, 8.91.

5aa: colorless prisms; mp 224–225 °C (from acetone); IR (KBr) 1726 cm^{-1}; ^{1}H-NMR (500 MHz, DMSO-d_6) δ: 3.84 (s, 3H, CO_2CH_3), 4.93 (d, *J* = 9.7, 1H, C3a-H), 5.81 (d, *J* = 9.7, 1H, C6a-H), 7.32 (brd, *J* = 7.7, 2H, ArH), 7.44–7.52 (m, 3H, ArH); ^{13}C-NMR (125 MHz, DMSO-d_6) δ: 52.9 (CO_2CH_3), 54.4 (C3a), 83.2 (C6a), 148.3 (C3), 158.8 (COO), 169.2 (NC=O), 171.1 (NC=O); HMRS (ESI) Calcd. for $C_{14}H_{14}N_2O_6Na$ (M^++CH_3OH+Na): 329.07496. Found: 329.07423. Anal. Calcd for $C_{13}H_{10}N_2O_5$: C, 56.94; H, 3.68; N, 10.22. Found: C, 56.58; H, 3.67; N, 10.12.

endo-**3ab**: pale yellow prisms; mp 110–114 °C (from $CHCl_3$); IR (KBr) 1732 cm^{-1}; ^{1}H-NMR (500 MHz, DMSO-d_6) δ: 2.73 (s, 3H, CH_3), 3.80 (s, 3H, CO_2CH_3), 3.88 (s, 3H, CO_2CH_3), 4.65 (d, *J* = 8.0, 1H, C3b-H), 5.71 (d, *J* = 8.0, 1H, C6a-H); ^{13}C-NMR (125 MHz, DMSO-d_6) δ: 25.2 (CH_3), 52.1 (C3b), 53.1 (CO_2CH_3), 54.8 (CO_2CH_3), 82.9 (*C*-COO), 85.6 (C6a), 155.0 (*C*OO), 162.9 (*C*OO), 170.5 (NC=O), 170.7 (NC=O), 178.0 (C=O); HMRS (ESI) Calcd. for $C_{12}H_{10}N_3O_9$ (M^+–H): 340.04170. Found: 340.03828.

4ab: colorless prisms; mp 210–211 °C (from acetone); IR (KBr) 1712 cm^{-1}; ^{1}H NMR (500 MHz, DMSO-d_6) δ 2.82 (s, 3H, CH_3), 3.76 (s, 3H, CO_2CH_3), 4.38 (d, *J* = 8.0, 1H, >CH-C(=O)), 5.33 (d, *J* = 8.0, 1H, -OCH-C(=O)); ^{13}C NMR (125 MHz, DMSO-d_6) δ 25.3 (CH_3), 53.9 (>*C*H-C(=O)), 54.8 (CO_2CH_3), 80.5 (-O*C*H-C(=O)), 83.7 (*C*-COO), 162.2 (COO), 171.3 (NC=O), 173.3 (NC=O), 183.0 (C=O); Anal. Calcd for $C_{17}H_{16}N_4O_{11}$: C, 45.14; H, 3.57; N, 12.39. Found: C, 45.40; H, 3.81; N, 12.25.

5ab: colorless prisms; mp 205–208 °C (from acetone-$CHCl_3$); IR (KBr) 1726 cm^{-1}; ^{1}H-NMR (500 MHz, DMSO-d_6) δ: 2.85 (s, CH_3, 3H), 3.83 (s, CO_2CH_3, 3H), 4.77 (d, *J* = 9.7, 1H, C3a-H), 5.65 (d, *J* = 9.7, 1H, C6a-H); ^{13}C-NMR (125 MHz, DMSO-d_6) δ: 25.1 (CH_3), 52.9 (C3a), 54.2 (CO_2CH_3), 83.0 (C6a), 148.2 (C3), 158.8 (COO), 170.2 (NC=O), 171.9 (NC=O); HMRS (ESI) Calcd. for $C_9H_{12}N_2O_6Na$ (M^++CH_3OH+Na): 267.05931. Found: 267.05428.

endo-**3ba**: colorless prisms; mp 249–252 °C (from acetone); IR (KBr) 1736 cm^{-1}; ^{1}H-NMR (500 MHz, DMSO-d_6) δ: 4.64 (d, *J* = 8.0, 1H, C3b-H), 5.90 (d, *J* = 8.0, 1H, C6a-H), 6.76 (d, *J* = 7.7, 2H, Ar-H), 7.26 (dd, *J* = 7.7, 7.5, 2H, Ar-H), 7.33 (dd, *J* = 7.5, 6.9, 1H, Ar-H), 7.52–7.60 (m, 6H, Ar-H), 7.72 (d, *J* = 7.7, 2H, Ar-H), 8.11 (dd, *J* = 6.9, 1.7, 2H, Ar-H); ^{13}C-NMR (125 MHz, DMSO-d_6) δ: 57.3 (C3b), 83.2 (C3a), 85.0 (C6a), 170.7 (NC=O), 171.6 (NC=O), 185.5 (C=O); Anal. Calcd for $C_{25}H_{17}N_3O_5$: C, 68.33; H, 3.90;

N, 9.56. Found: C, 68.32; H, 3.76; N, 9.40.

exo-**3ba**: colorless prisms; mp 215–216 °C (from acetone); IR (KBr) 1714 cm^{-1}; ^{1}H-NMR (500 MHz, DMSO-d_6) δ: 4.83 (d, J = 8.0, 1H, C3b-H), 5.68 (d, J = 8.0, 1H, C6a-H), 6.66 (dd, J = 7.5, 1.7, 2H, Ar-H), 7.39 (d, J = 7.5, 3H, Ar-H), 7.48 (d, J = 7.5, 3H, Ar-H), 7.79 (d, J = 7.5, 2H, Ar-H), 7.59 (d, J = 8.6, 3H, Ar-H), 8.30 (dd, J = 8.6, 1.7, 2H, Ar-H); ^{13}C-NMR (125 MHz, DMSO-d_6) δ: 56.2 (C3b), 78.5 (C6a), 84.2 (C3a), 169.2 (NC=O), 169.4 (NC=O), 188.6 (C=O); HMRS (ESI) Calcd. for $C_{26}H_{21}N_3O_6Na$ (M^++CH_3OH+Na): 494.13280. Found: 494.13262.

endo-**3bb**: colorless prisms; mp 249–252 °C (from *n*-hexane-AcOEt); IR (KBr) 1736 cm^{-1}; ^{1}H-NMR (500 MHz, DMSO-d_6) δ 2.58 (s, 3H, CH_3), 4.49 (d, J = 8.0, 1H, C3b-H), 5.71 (d, J = 8.0, 1H, C6a-H), 7.50–7.57 (m, 6H, Ar-H), 7.66 (d, J = 7.5, 2H, Ar-H), 7.99–8.01 (m, 2H, Ar-H); ^{13}C-NMR (125 MHz, DMSO-d_6) δ 24.8 (CH_3), 57.0 (C3b), 82.9 (C3a), 84.8 (C6a), 171.4 (NC=O), 171.5 (NC=O), 185.2 (C=O); HMRS (ESI) Calcd. for $C_{20}H_{15}N_3O_5Na$ (M^++Na): 400.09094. Found: 400.08871.

exo-**3bb**: colorless prisms; mp 210–211 °C (from acetone); IR (KBr) 1720 cm^{-1}; ^{1}H-NMR (500 MHz, DMSO-d_6) δ: 2.59 (s, 3H, CH_3), 4.62 (d, J = 8.0, 1H, C3b-H), 5.48 (d, J = 8.0, 1H, C6a-H), 7.39–7.43 (m, 3H, Ar-H), 7.57–7.58 (m, 3H, Ar-H), 7.68–7.70 (m, 2H, Ar-H), 8.27 (dd, J = 7.7, 1.7, 2H, Ar-H); ^{13}C-NMR (125 MHz, DMSO-d_6): δ 24.7 (CH_3), 56.2 (C3b), 78.7 (C3a), 83.4 (C6a), 169.8 (NC=O), 170.0 (NC=O), 189.3 (C=O); Anal. Calcd for $C_{20}H_{15}N_3O_5$: C, 63.66; H, 4.01; N, 11.14. Found: C, 63.73; H, 4.28; N, 10.87.

Crystal structure analysis – The single crystals for inclusion complexes were prepared by slow evaporation of solution at room temperature. All measurements were performed on RAXIS RAPID imaging plate area detector with graphite-monochromated Mo-Kα radiation (λ=0.7107 Å). The data were collected at a temperature of 23 ± 1 °C to a maximum 2θ value of 55°. The structure was solved by direct method (SIR92[13a]), and all hydrogen atoms were located at calculated positions. The structure was refined by a full-matrix least-squares technique using anisotropic thermal parameters for non-hydrogen atoms and a riding model for hydrogen atoms. All calculations were performed using the crystallographic software package Crystal Structure.[13b,c] These X-ray crystallographic data have been deposited at the Cambridge Crystallographic Data Centre (CCDC). Crystal data of *anti-endo-endo*-**4aa**: $C_{27}H_{20}N_4O_{11}$•C_3H_6O (**4aa**+acetone), M=634.55, monoclinic, Space group $P2_1/c$, a=9.635 (1), b=11.409 (2), c=26.545 (1) Å, β=94.297 (8) °, V=2909.7 (6) $Å^3$, D_c=1.448 g cm^{-3}, Z=4, R=0.057, R_w=0.100. CCDC ref. No. 695559; **5ab**: $C_8H_8N_2O_5$, M=212.16, orthorhombic, Space group *Pbca*, a=14.402 (4), b=13.171 (4), c=9.650 (4) Å, V=1830 (1) $Å^3$, D_c=1.583 g cm^{-3}, Z=8, R=0.042, R_w=0.044, CCDC ref. No. 696187; *endo*-**3bb**: $C_{20}H_{15}N_3O_5$, M=377.36, monoclinic, Space group *P21/n*, a=10.193 (2), b=10.496 (2), c=16.406 (3) Å, β=92.247 (6) °, V=1750.4 (5) $Å^3$, D_c=1.432 g cm^{-3}, Z=4, R=0.090, R_w=0.135, CCDC ref. No. 908115.

Measurement of visible absorption spectra – Solutions of **1a** (2.9 mmol/L), **2a** (3.8 mmol/L), and **3a** (3.7 mmol/L) in $CHCl_3$ were used for the measurement at 25 °C.

Molecular orbital (MO) calculations – The MO calculations were performed by density functional theory (DFT) based *ab initio* method at the B3LYP/6-31G(d) level using Gaussian09 program package.[6] Vibrational frequencies were used to characterize the nature of the stationary points. Zero point energy (ZPE) corrections were scaled by 0.9804.[14]

ACKNOWLEDGEMENTS

We thank Ms. R. Haraguchi and Mr. K. Egami for experimental assistance.

REFERENCES AND NOTES

1. a) M. Eto, K. Harano, Y. Yoshitake, and T. Hisano, *J. Heterocycl. Chem.*, 1993, **30**, 1557; b) M. Eto, Y. Yoshitake, K. Harano, and T. Hisano, *J. Chem. Soc., Perkin Trans. 2*, 1994, 1337; c) Y. Yoshitake, M. Eto, and K. Harano, *Heterocycles*, 1997, **45**, 1873; d) Y. Yoshitake, M. Eto, and K. Harano, *Tetrahedron Lett.*, 1998, **39**, 2761; e) Y. Yoshitake, M. Eto, and K. Harano, *Chem. Pharm. Bull.*, 1999, **47**, 601; f) K. Yamaguchi, Y. Yoshitake, and K. Harano, *Heterocycles*, 2009, **78**, 2777; g) K. Yamaguchi, M. Eto, Y. Yoshitake, and K. Harano, *J. Phys. Org. Chem.,* 2013, *in press*.
2. a) J. P. Freeman, J. J. Gannon, and D. L. Surbey, *J. Org. Chem.*, 1969, **34**, 187; b) J. P. Freeman and M. L. Hoare, *J. Org. Chem.*, 1971, **36**, 19; c) A. Kotali and V. P. Papageorgiou, *Org. Prep. Proced. Int.*, 1991, **23**, 611; d) A. Kotali and P. G. Tsoungas, *Heterocycles*, 1989, **29**, 1615.
3. a) M. Nishio, M. Hirota, and Y. Umezawa, *The CH/π interaction; Evidence Nature and Consequences*, Wiley, New York, 1998; b) O. Takahashi, Y. Kohno, and M. Nishio, *Chem. Rev.*, 2010, **110**, 6049; c) M. Nishio, *Phys. Chem. Chem. Phys.*, 2011, **13**, 13873.
4. R. Sustmann, *Tetrahedron Lett.*, 1971, **12**, 2717, 2721.
5. The *endo*/*exo* stereochemistries of **3ba** and **3bb** were determined by analysing the NOE (nuclear Overhauser effect) data. In the case of *endo*-**3bb**, which was subjected to single crystal X-ray analysis, the protons of the phenyl group attached to the C3a position correlated to the C3b methine proton. However, such a correlation was not observed in the case of *exo*-**3bb**.
6. Gaussian 09, Revision A.1, M. J. Frisch, G. W. Trucks, H. B. Schlegel, G. E. Scuseria, M. A. Robb, J. R. Cheeseman, G. Scalmani, V. Barone, B. Mennucci, G. A. Petersson, H. Nakatsuji, M. Caricato, X. Li, H. P. Hratchian, A. F. Izmaylov, J. Bloino, G. Zheng, J. L. Sonnenberg, M. Hada, M. Ehara, K. Toyota, R. Fukuda, J. Hasegawa, M. Ishida, T. Nakajima, Y. Honda, O. Kitao, H. Nakai, T. Vreven, J. A. Montgomery, Jr., J. E. Peralta, F. Ogliaro, M. Bearpark, J. J. Heyd, E. Brothers, K. N. Kudin, V. N. Staroverov, R. Kobayashi, J. Normand, K. Raghavachari, A. Rendell, J. C. Burant, S. S. Iyengar,

J. Tomasi, M. Cossi, N. Rega, J. M. Millam, M. Klene, J. E. Knox, J. B. Cross, V. Bakken, C. Adamo, J. Jaramillo, R. Gomperts, R. E. Stratmann, O. Yazyev, A. J. Austin, R. Cammi, C. Pomelli, J. W. Ochterski, R. L. Martin, K. Morokuma, V. G. Zakrzewski, G. A. Voth, P. Salvador, J. J. Dannenberg, S. Dapprich, A. D. Daniels, Ö. Farkas, J. B. Foresman, J. V. Ortiz, J. Cioslowski, and D. J. Fox, Gaussian, Inc., Wallingford CT, 2009. The calculation data (atomic coordinates) are available upon request (e-mail address: meto@ph.sojo-u.ac.jp).

7. *exo*-**3ca**: E=–849.3030 (E_{ZPE}=–849.1309) hartree; *endo*-**3ca:** –849.2979 (E_{ZPE}=–849.1258) hartree.
8. a) R. Taylor and O. Kennard, *J. Am. Chem. Soc*., 1982, **104**, 5063; b) G. R. Desiraju, *Acc. Chem. Res*., 1991, **24**, 290; c) G. R. Desiraju, *Acc. Chem. Res*., 1996, **29**, 441; d) T. Steiner, J. A. Kanters, and J. Kroon, *J. Chem. Soc., Chem. Commun*., 1996, 1277; e) T. Steiner, *Cryst. Rev*., 1996, **6**, 1; f) T. Steiner, *Angew. Chem. Int. Ed*., 2002, **41**, 48.
9. In the TS structures from **1b** and **2b** without CH/O interaction, there is almost no energy difference between the *exo*-TS and *endo*-TS [*exo*-TS : E=–1311.3626 (E_{ZPE}=–1311.0252) hartree; *endo*-TS : see Figure 4].
10. Calculations of the *endo*-TS for the reaction of **1a** with **2a** by B3LYP/6-31G(d) suggested the presence of steric interference between the ester and the phenyl groups. In comparison to the TS for the reaction of **1a** with **2b**, the distance between the nitrogen of maleimide and the nitrogen of >C=N→O moiety is separated by ca. 0.14 Å.

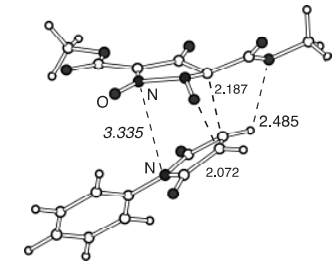

11. The B3LYP/6-31G(d) calculation for the rotation model without CH/O interaction also gave stationary point [E=–1703.7515 (E_{ZPE}=–1703.3830) hartree].
12. Similar interactions are also observed in Diels-Alder reactions. The B3LYP/6-31G(d) calculated TS structures for the cycloaddition of 2,5-bis(methoxycarbonyl)-3,4-diphenylcyclopentadienone with **2b** indicate that the *endo*-TS is stabilized by the O/H-C interactions not only between the ester carbonyl oxygen and the 2'-hydrogen of the phenyl group (Ph-H•••O= 2.473Å) but also between the proton of **2b** and the ester ether oxygen (CH•••O< 2.409Å). The *endo*-TS energy was ca. 2.1 kcal/mol more stable than that of *exo*-TS. Detailed study is in progress.

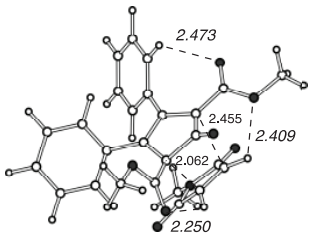

endo-TS
E= –1584.6854 hartree

13. a) SIR2008: M. C. Burla, R. Caliandro, M. Camalli, B. Carrozzini, G. Cascarano, L. De Caro, C. Giacovazzo, G. Polidori, D. Siliqi, and R. Spagna, *J. Appl. Cryst*., 2007, **40**, 609; b) CrystalStructure 4.0: Crystal Structure Analysis Package, Rigaku Corporation (2000–2010). Tokyo 196-8666, Japan.
14. A. P. Scott and L. Radom, *J. Phys. Chem*., 1996, **100**, 10502.